Agriculture and Environment, 7 (1982) 161—174
Elsevier Scientific Publishing Company, Amsterdam — Printed in The Netherlands

TRANSPORT AND FIXATION OF PHOSPHATE IN ACID, HOMOGENEOUS SOILS

II. COMPUTER SIMULATION

P. DE WILLIGEN, P.A.C. RAATS and R.G. GERRITSE

Institute for Soil Fertility, Postbus 30003, 9750 RA Haren (Gn..) (The Netherlands)

(Accepted 19 October 1981)

ABSTRACT

De Willigen, P., Raats, P.A.C. and Gerritse, R.G., 1982. Transport and fixation of phosphate in acid, homogeneous soils. II. Computer simulation. *Agric. Environm.*, 7: 161—174.

Results of computer simulation concerning transport, nonlinear adsorption, and fixation of orthophosphate in soil, based on a physico-mathematical model discussed in Part I, are presented. The consequences of application of excessive amounts of phosphate and the influence on long-term effects of fixation rate, adsorption isotherm, time of application, and equilibrium concentration were investigated. The fixation rate was found to have the greatest influence on depth of penetration. In the limiting case of very high fixation rates it was shown that the analytical solutions derived in Part I can be used to predict rate of penetration.

INTRODUCTION

The purpose of this series of three papers is to evaluate the effects of surplus phosphate addition on the basis of: (a) a model describing the transport; (b) column experiments; and (c) associated batch experiments to determine the adsorption isotherm and the rate of fixation.

In Part I (Raats et al., 1982), a physico-mathematical model was formulated and analytical solutions for some limiting cases were derived. However, the nonlinearity of both the adsorption isotherm and the rate of fixation makes it difficult to find a complete analytical solution, even for the simplest case of a constant input. Therefore, a computer program was written to solve the problem numerically. In this paper (Part II) the computer program is described and some examples of calculations based on measured adsorption isotherms of two soils and several assumed values of the rate of fixation are presented. The analytical solutions derived in the first paper are used in interpreting the results of the calculations. In Part III (Gerritse et al., 1982) results of batch experiments will be used in the computer program and will be compared with results of column experiments.

0304-1131/82/0000—0000/$02.75

THE COMPUTER PROGRAM

The computer implementation of the physico-mathematical model introduced in Part I is in outline similar to a model developed by De Wit and Van

TABLE I

Inputs and some estimates related to saturating fronts

Run No.		I	II	III	IV	V	VI
A. Inputs							
Soil[a]		l.s.	l.s.	b.c.	l.s.	l.s.	l.s.
Bulk density (g cm^{-3})		1.1	1.1	1.2	1.1	1.1	1.1
Available % Al + Fe		0.1+0.1	0.5+0.5	0.5+0.5	0.1+0.1	0.1+0.1	0.1+0.1
Initial half-life (year)	0.02	a	a	a			
(a, b, c, d refer to	0.2	b	b	b	a		
Figs. 2—7.)	2	c	c	c	b		
	20	d	d	d			
Net application of P (kg ha^{-1} $year^{-1}$)[b]		115	115	115	115	115	115
Water supply (mm day^{-1})		1	1	1	1	1[b]	1[b]
Volumetric water content (ml cm^{-3})		0.25	0.25	0.25	0.25	0.25	0.25
Dispersion coefficient (cm^2 day^{-1})		0.468	0.468	0.468	0.468	0.468	0.468
Initial level of P (mg ml^{-1})							
solution[c]	c	0.0001	0.0001	0.0001	0.0010	0.0001	0.0001
mobile	μ	0.0083	0.0083	0.0826	0.0506	0.0083	0.0083
immobile	σ	0.1037	0.1037	0.1037	0.0614	0.1037	0.1037
total	$\mu+\sigma$	0.1120	0.1120	0.1863	0.1120	0.1120	0.1120
B. Sharp front approximations							
Level of P behind front (mg l^{-1})							
solution		0.03	0.03	0.03	0.03		
mobile		0.189	0.189	0.45	0.189		
immobile		1.38	6.92	6.92	1.38		
total		1.57	7.11	7.37	1.57		
Capacity = level behind front – initial level							
solution		0.0315	0.0315	0.0315	0.306		
mobile		0.18	0.18	0.363	0.14		
immobile		1.2802	6.8159	6.8159	1.3225		
total		1.46	6.9959	7.1789	1.4619		
Speed of front (cm $year^{-1}$)		0.788	0.164		0.787		

[a] l.s. = light sand; b.c. = basin clay.

[b] The P is applied annually on 30 March, except that:
(1) in Run V the application is stopped when the phosphate in the soil solution at a depth of 50 cm reaches 0.0003 mg ml^{-1}; and

[c] (2) in Run VI the annual application is varied between 31 March, 30 June, 30 September, and 31 December.

The equilibrium concentration of the immobilisation reaction(s) is assumed to be 0.0001 mg ml^{-1}, except in Run IV where it is assumed to be 0.001 mg ml^{-1}.

Keulen (1972), a copy of the program is available upon request. The inputs for six different runs are summarized in Part A of Table I. In the program, a physically and chemically homogeneous soil column, 100 cm long and of 1 cm^2 cross section, is divided in 20 layers of 5 cm. Immediately following each annual P application of 140 kg ha^{-1}, corresponding to an overdose of 100 t pig slurry per ha, of which 25 kg ha^{-1} is assumed to be immediately

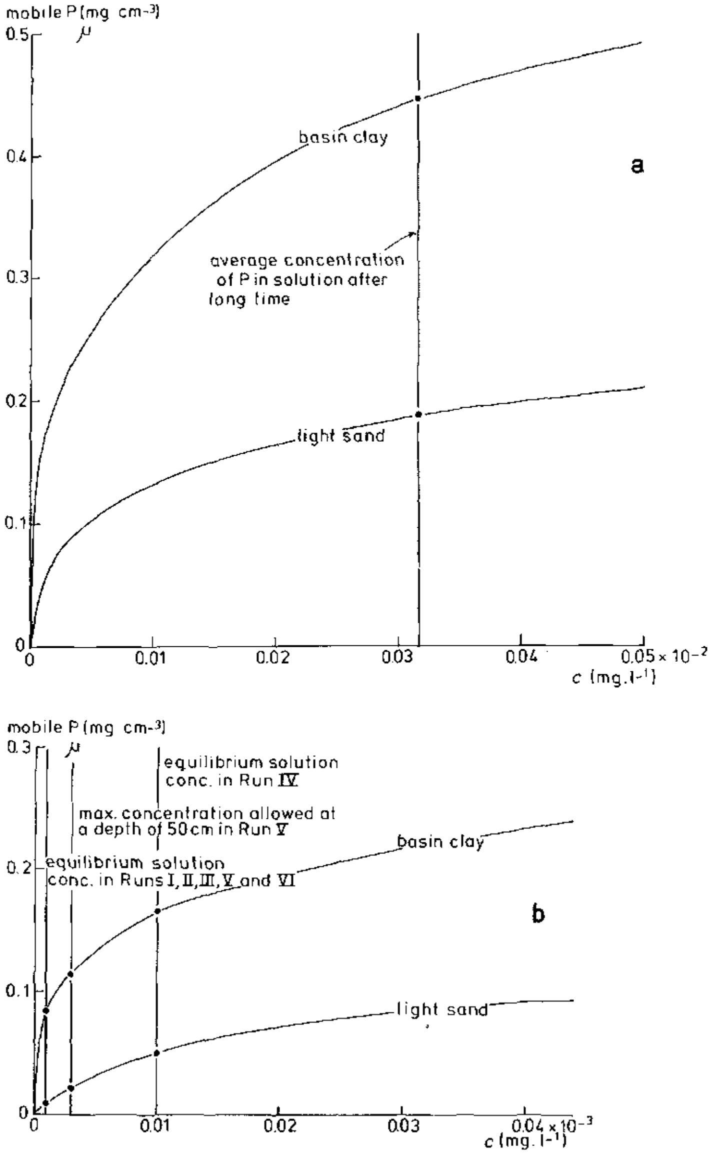

Fig. 1a and b. Relation between mobile phosphate (μ) and concentration (c) for two Dutch soils. A part of Fig. 1a is magnified in Fig. 1b.

taken up by the crop, the top 20 cm of the soil profile is assumed to be mixed thoroughly. The time step is 5 days. The dispersion coefficient is corrected for numerical dispersion. The two soils used in the calculations are a light sand (l.s.) and a basin clay (b.c., "komklei" in Dutch) with bulk densities of 1.1 and 1.2 g cm^{-3}. The relationships between μ and c for the two soils shown in Fig. 1 are calculated on the basis of equation (2) of Part I, the adsorption isotherms of fig. 1 of Part I, the bulk densities, and a constant water content of 0.25 ml cm^{-3}. The curves of Fig. 1 are introduced in the program as a table of coordinate pairs. From this table, c is obtained as a function of μ by interpolation.

The percentage of available Al and Fe, the initial half-lives, the net application of P, and the initial level of P in the soil are all chosen in accordance with the values and ranges discussed in Part I. Run I is the main reference. In Run II the influence of increasing the percentage available Al + Fe is considered. In Run III the percentage available Al + Fe is also large and the adsorption isotherm for the light sand is replaced by the one for the basin clay. In Run IV a higher initial level of P is considered. In Run V the application is stopped when the concentration in the soil solution at a depth of 50 cm reaches 3×10^{-4} mg ml^{-1}.

TABLE II

Cumulative precipitation and evaporation

Date	Time interval (days)	Cumulative precipitation[a] (mm)	Cumulative evaporation (mm)
16–4	0	0	0
1–5	15	28	35
16–5	30	62	80
1–6	46	99	120
16–6	61	141	170
1–7	76	182	220
16–7	91	223	270
1–8	107	264	318
16–8	122	300	360
1–9	138	348	405
16–9	153	384	440
1–10	168	429	460
1–11	199	504	480
1–12	229	582	484
1–1	260	651	485
1–2	291	725	486
1–3	319	788	494
1–4	350	846	514
16–4	365	882	534
1–5	380	910	569

[a] 75% probability that the cumulative precipitation will be smaller than this amount.

In Runs I—V the excess precipitation is assumed to be 1 mm day^{-1}. In The Netherlands the average excess precipitation over evapotranspiration is 300—400 mm year^{-1}, so averaged over the year there is below the root zone a downward flux of about 1 mm day^{-1}. Table II shows the cumulative evapotranspiration and precipitation for a wet year in The Netherlands (Rijtema and Bon, 1974). The probability of a cumulative rainfall lower than shown in Table II is 75%. In Run VI precipitation and evapotranspiration are distributed within a year as shown in Table II and the annual application is varied between 31 March, 30 June, 30 September and 31 December.

Summarizing, the computer program generally solves the partial differential equations:

$$\frac{\delta\mu}{\delta t} = -\theta v\frac{\delta c}{\delta z} + \theta D\frac{\delta^2 c}{\delta z^2} - \frac{\delta\sigma}{\delta t} + I(365, t)A \qquad 0 < z < z_1 \tag{1}$$

$$\frac{\delta\mu}{\delta t} = -\theta v\frac{\delta c}{\delta z} + \theta D\frac{\delta^2 c}{\delta z^2} - \frac{\delta\sigma}{\delta t} \qquad z_1 < z < \infty \tag{2}$$

$$\frac{\delta\sigma}{\delta t} = (1 - \sigma/\sigma_\infty)k(\mu - \mu_e) \qquad 0 < z < \infty \tag{3}$$

where μ, b, c, z, θ, v, t, σ_∞, D, k, and μ_e have the same meaning as in Part I; z_1 is the thickness of the plow layer (cm); A the net application rate in mg cm^{-3} day^{-1}, and $I(365, t)$ denotes a periodic Dirac delta function defined by:

$$I(365, t) = \begin{cases} 1 & \text{for } t = 365k,\ k = 0, 1, 2, \ldots \\ 0 & \text{elsewhere} \end{cases} \tag{4}$$

The initial and boundary conditions employed are:

$$\mu = \mu_i = \mu_e \qquad c = c_i = c_e \qquad \sigma = \sigma_i \qquad \text{for } z > 0,\ t = 0 \tag{5}$$

$$vc - D\frac{\delta c}{\delta z} = 0 \qquad \text{for } z = 0,\ t > 0 \tag{6}$$

$$\lim_{z\to\infty}\frac{\delta c}{\delta z} = 0 \tag{7}$$

RESULTS

Sharp front approximation

For all the Runs listed in Table I the equilibrium state and the initial state coincide. In Part I it was made plausible that eventually there will be three zones, viz., (a) a transmission zone near the soil surface in which all the available Al + Fe has been used so that $\sigma = \sigma_\infty$, and in which c, μ, and F have reached their average ultimate values c_∞, μ_∞, and $\theta v c_\infty$; (b) a fixation front moving down at a velocity v_F, having a constant shape, and the flux F_r of orthophosphate with respect to the fixation front having a certain constant value; (c) an equilibrium zone in which c, μ, σ, and F have the values c_e, μ_e, $\sigma_e = \sigma_i$, and $F = F_e = \theta v c_e$. When the equilibrium state and the initial state coincide, then equations (25) and (26) of Part I with $c_e = c_i$, $\mu_e = \mu_i$, and $\sigma_e = \sigma_i$ are the appropriate expressions for the velocity of the fixation front and for the flux relative to the fixation front.

With the assumptions introduced in the computer model and for the limiting case with instantaneous fixation, two periods can be distinguished. During the first period a fraction $(F_\infty - F_i)/F_\infty$ of the added orthophosphate will be immobilized in the top 20 cm and a fraction F_i/F_∞ will move into the subsoil. During the second period there will be at all times near the soil surface a zone in which all the Al and Fe available for binding P has been used. A sharp fixation front will separate this region from the region in which the initial distribution of P still prevails. In the zone where all the available Al + Fe is spent, the concentration $\bar{c}_\infty$ of phosphate in solution, averaged over the entire year, is given by:

$$\bar{c}_\infty = \frac{\bar{F}[z=0]}{R - \mathrm{ET}} \tag{8}$$

where $\bar{F}[z=0]$ is the annual application of phosphate, and $R - \mathrm{ET}$ is the average excess precipitation over evapotranspiration. The amount $\bar{\mu}_\infty$ of mobile phosphate averaged over the entire year can be read approximately from the adsorption isotherm, as is shown in Fig. 1b. In view of the non-linearity of the adsorption isotherm, the value of $\bar{\mu}_\infty$ will depend on the entire annual time course of the concentration in the soil solution. However, if the fluctuations are not very large, then the value of μ corresponding to $\bar{c}_\infty$ on the adsorption isotherm will be a reasonable estimate of $\bar{\mu}_\infty$.

For each Run, in Part B of Table I the levels of P are listed together with the capacities for holding P in the various phases of the P saturated zone and the speed of the sharp front.

Run I: reference case

Figs. 2a, b, c, and d show, respectively, for initial half-lives 0.02, 0.2, 2, and 20 years the resulting profiles of immobile P after 10, 20, 30, 50, 100 years. According to Table IB the frontal speed for Run I is 0.788 cm year^{-1}. This agrees closely with the results shown in Fig. 2c for rapid immobilisation with $\tau_{1/2} = 0.02$ year; it takes about 25 years for the tilled layer of 20 cm to fill up, and after 100 years the front has reached a depth of about 80 cm.

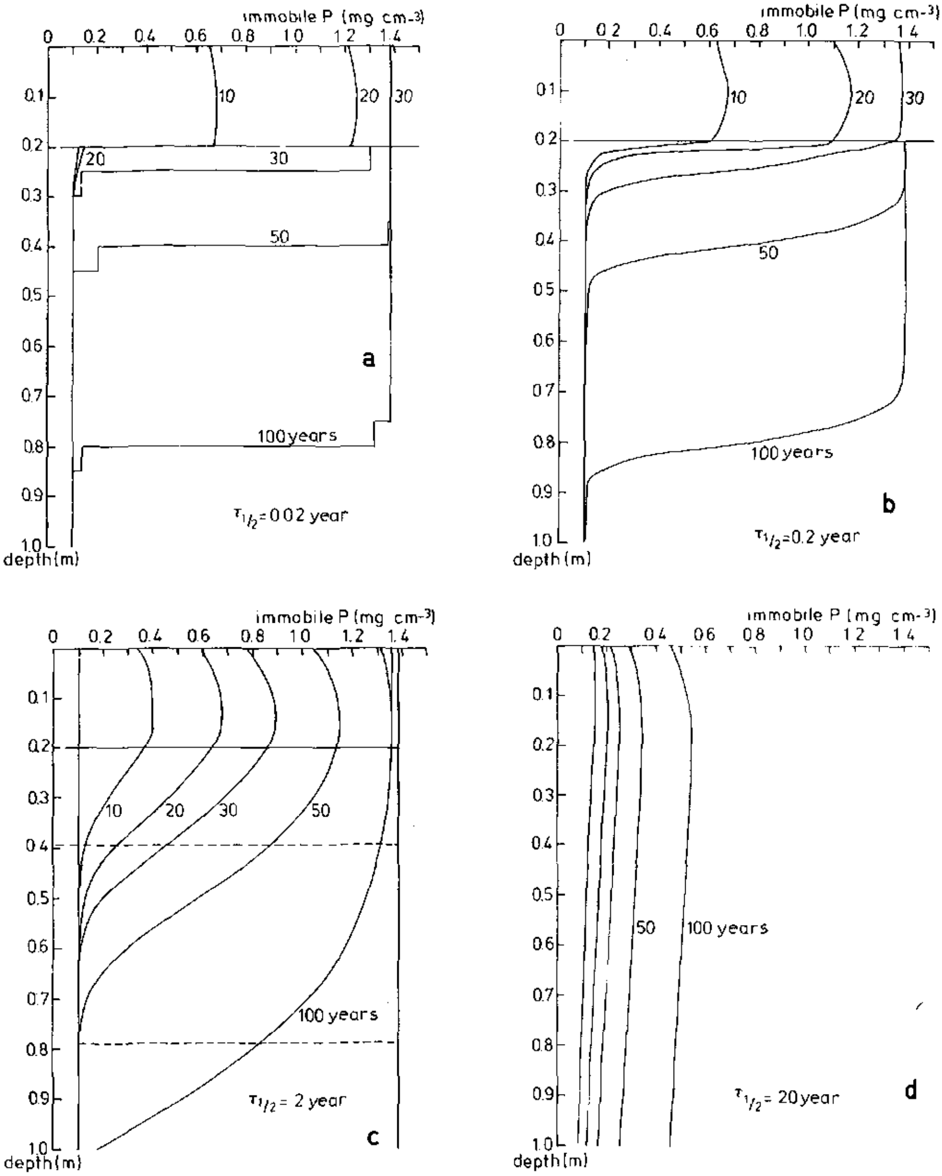

Fig. 2a—d. Development of profiles of immobile phosphate for different half-lives of fixation rate. Run I.

The results in Figs. 2b, c and d show that with lower rates of immobilisation the front becomes more diffuse. For $\tau_{1/2}$ = 0.2 year the sharp front approximation is still quite accurate, but for $\tau_{1/2}$ = 2 years the penetration of immobile P beyond the estimated depth of the sharp front is very significant. For example, after 50 years the leading edge of the diffuse front has reached a depth of about 70 cm, whereas the corresponding sharp front is located at about 40 cm. This deeper penetration of immobile P may lead to an increase of the concentration of P in the drainage water. For $\tau_{1/2}$ = 20 years the leading edge of the diffuse front has already reached a depth of 70 cm after 10 years.

Figs. 3a, b, c, and d show the corresponding profiles of the concentration

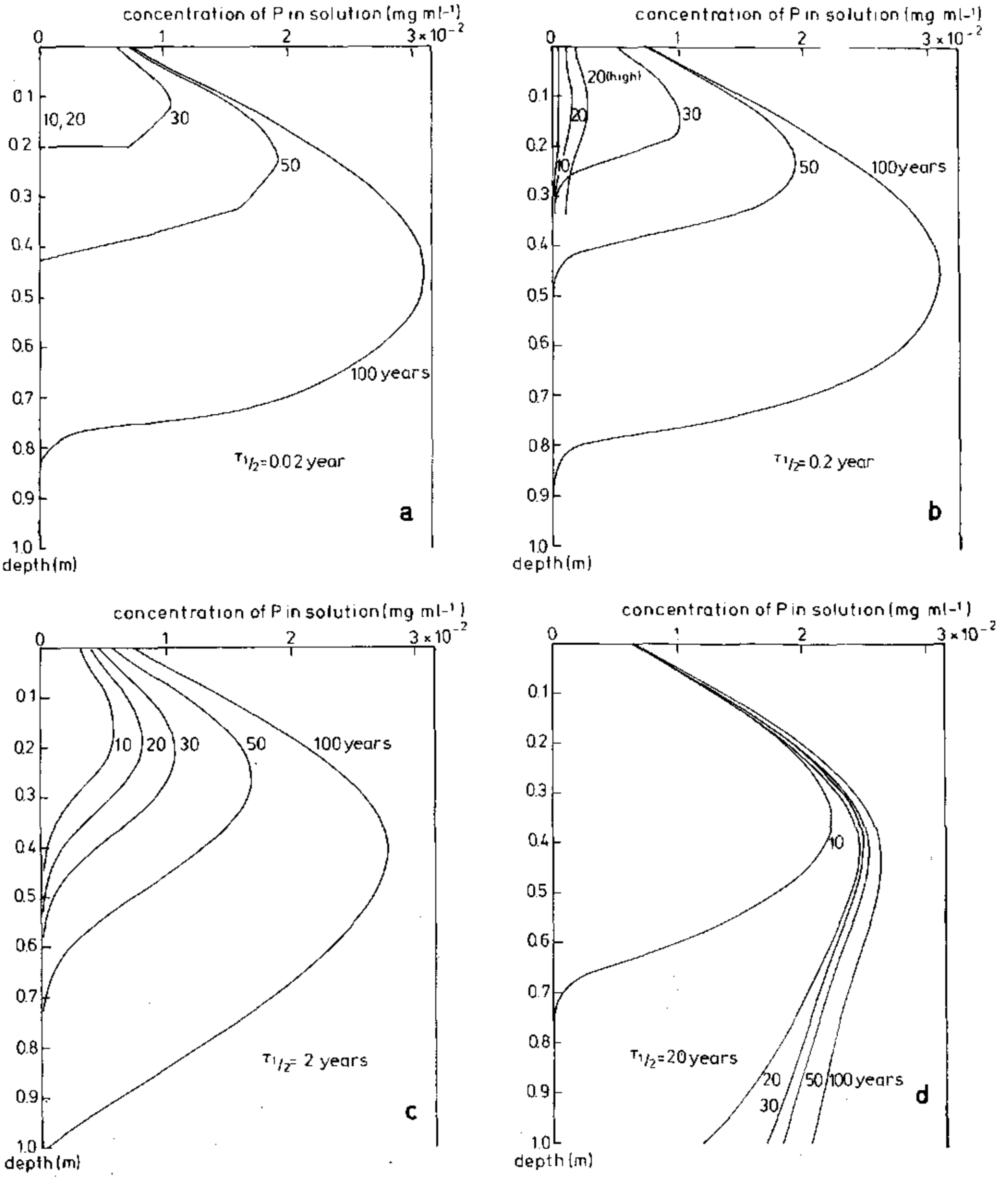

Fig. 3a–d. Development of profiles of phosphate concentration in the soil solution for different half-lives of fixation rate. Run I.

of P in the soil solution immediately before the next application of 115 kg ha^{-1}. Due to leaching of mobile P in the course of the year the concentration at the soil surface is relatively low. However, the thorough mixing of the top 20 cm following each annual P application will cause the distribution of immobilised P in the top 20 cm to remain uniform.

Figs. 4a, b, c, and d show plots of $\int_0^t c\,dt$, the exposure to phosphate in the soil solution, as a function of depth and time for $\tau_{1/2}$ = 0.02, 0.2, 2, and 20 years, respectively. The results for $\tau_{1/2}$ = 0.02 and 0.2 years are virtually identical. For $\tau_{1/2}$ = 2 and 20 years the influence of the wider spread becomes noticeable.

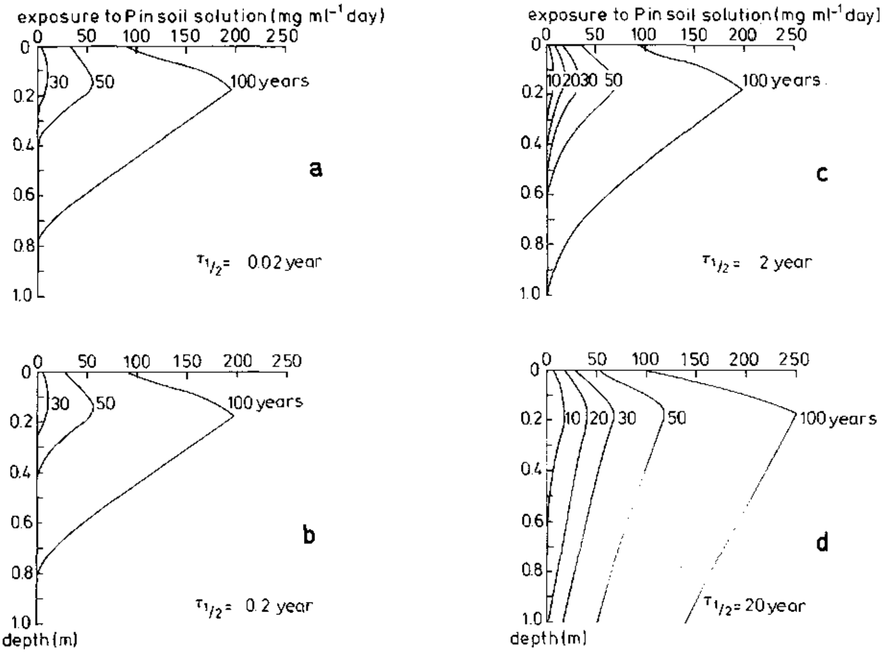

Fig. 4a—d. Exposure to phosphate in soil solution, for different half-lives of fixation rate. Run I.

Run II: larger fixation capacity

In Run II the percentages of available Al and Fe are 0.5%; all other inputs are the same as in Run I. Some of the results are shown in Figs. 5a, b, c, and d. The speed of the saturating front is 0.164 cm year^{-1}. Hence, it will take 122 years to fill up the tilled layer of 20 cm. Yet even for $\tau_{1/2}$ = 0.2 year there is a small leakage to the layer 20—25 cm, and for $\tau_{1/2}$ = 2 years after 50 years the leading edge is at a depth of about 50 cm. The protection provided by a higher percentage of available Fe + Al is significant only if at the same time the initial rate of immobilisation also increases. It would, of course, be reasonable to assume that the initial rate of immobilisation increases in proportion with the percentage of available Al + Fe.

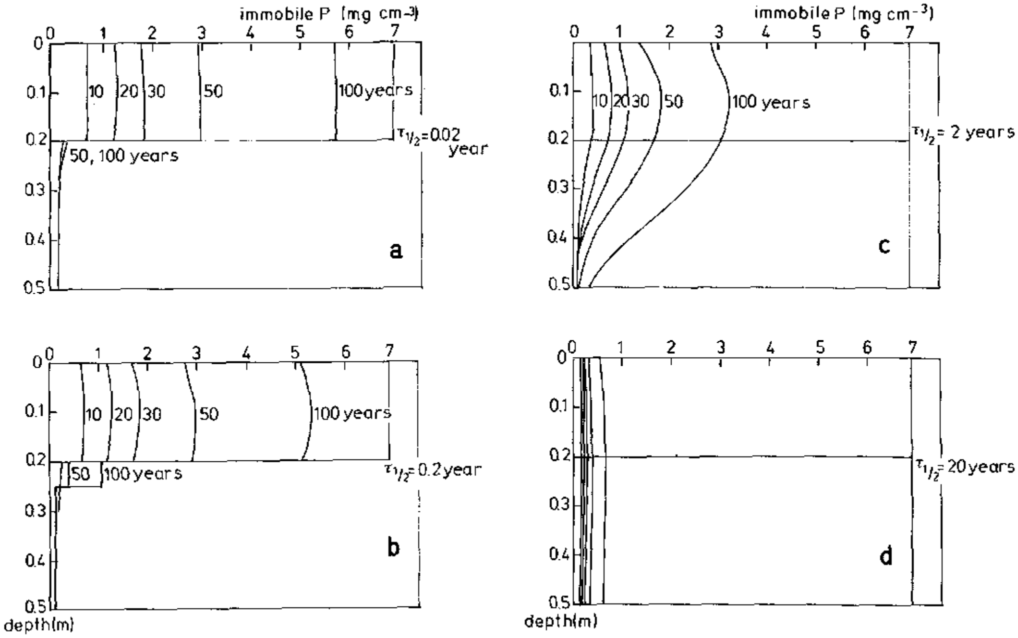

Fig. 5a—d. As fig. 2. Results of Run II.

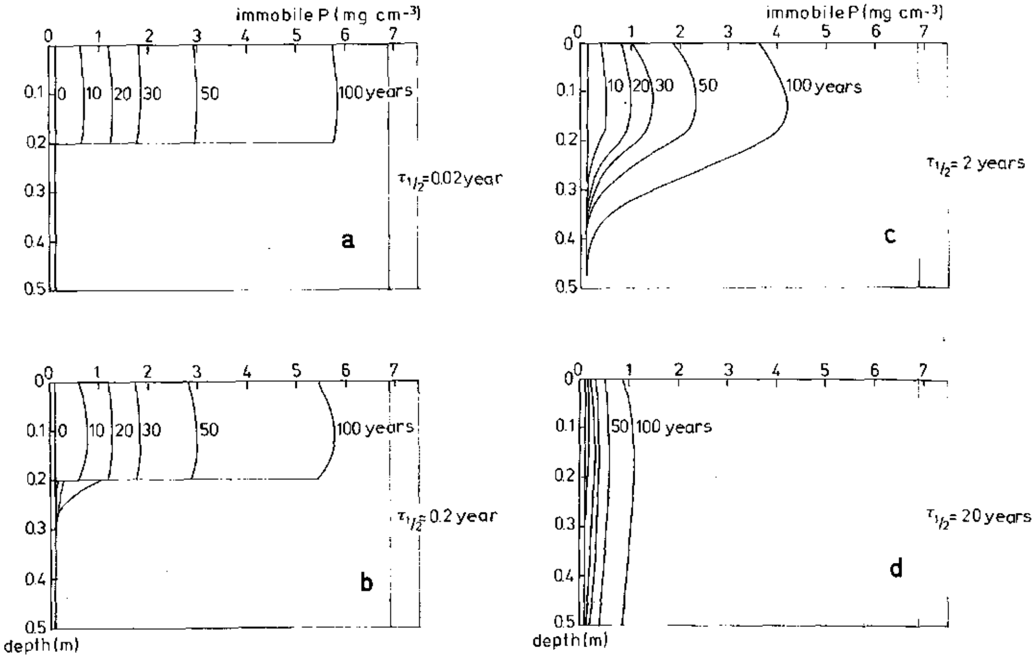

Fig. 6a—d. As fig. 2. Results of Run III.

Run III: larger fixation capacity and larger adsorption capacity

As in Run II, the percentages of available Al and Fe are 0.5%, but the adsorption isotherm for the light sand used in Runs I and II is replaced by the one for the basin clay.

Comparison of Figs. 6a, b, c, and d with Figs. 5a, b, c, and d shows that the stronger adsorption causes an increase of the immobilisation near the soil surface, particularly for $\tau_{1/2}$ = 2 and 20 years.

Run IV: higher equilibrium concentration

In Run IV the equilibrium concentration is 0.001 mg ml^{-1}; otherwise all inputs are the same as in Run I. The resulting change of the speed of the saturating front is negligible, but comparison of Figs. 7a and b with Figs. 2a and b shows that the fronts become wider. For example, for $\tau_{1/2}$ = 2 years the leading edges of the successive fronts are between 20 and 30 cm deeper in Run IV than in Run I.

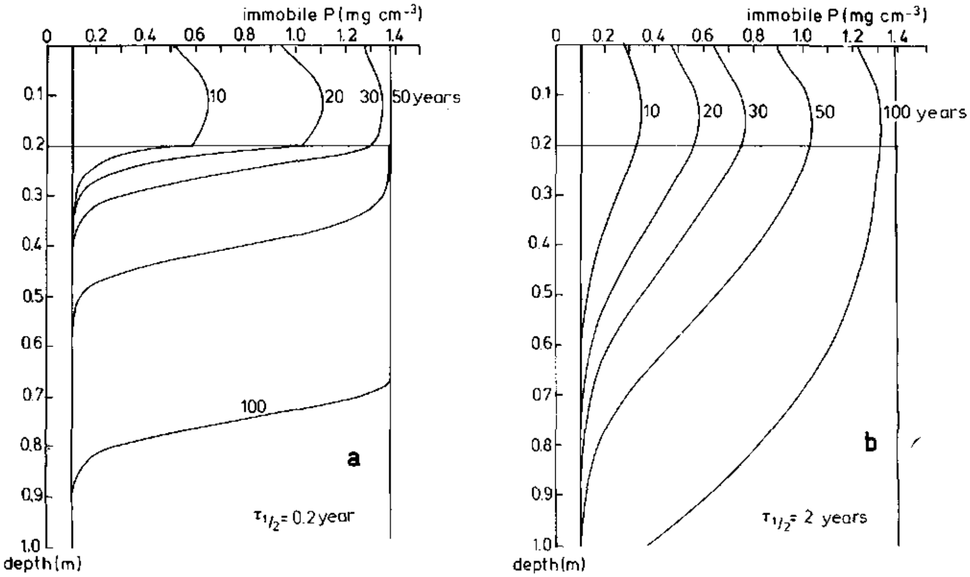

Fig. 7a—b. As fig. 2. Results of Run IV.

Run V: limited duration of exposure

Fig. 8a shows the time courses of the concentration at a depth of 50 cm when the disposal is stopped as soon as the concentration of P in solution becomes 3×10^{-4} mg P ml^{-1}. Due to mobile solute present in the zone 0—50 cm depth the concentration continues to rise for some time. Fig. 8b shows the response at a depth of 25 cm. There the overshoot is of much shorter duration.

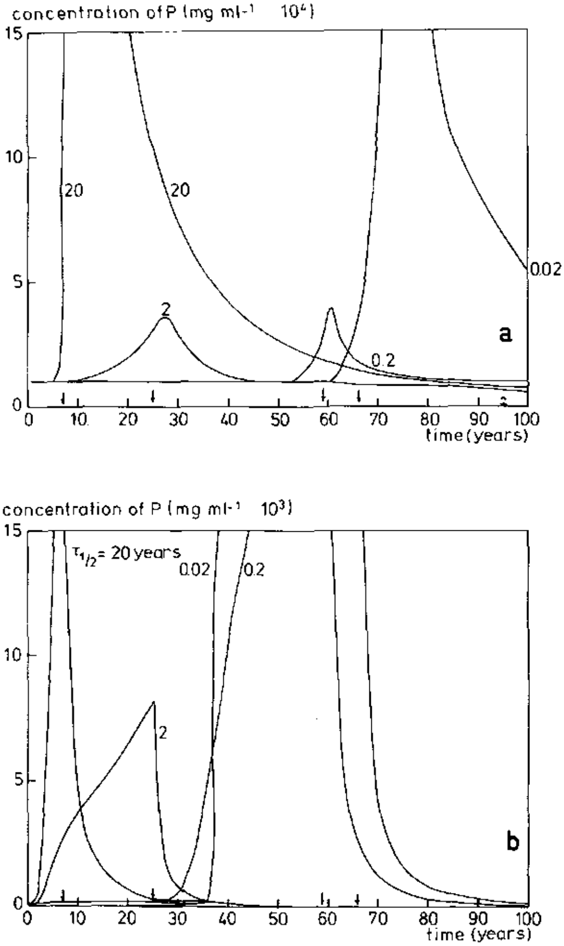

Fig. 8a—b. Course of concentration of phosphate in soil solution with time at depths of: (a) 50 cm; and (b) 25 cm. Disposal of phosphate at the surface was stopped as soon as the concentration at 50 cm exceeded 3×10^{-4} mg ml^{-1} (indicated by arrows). Run V.

Run VI: fluctuating water movement and variation of the timing of P disposal

In Run V the excess rainfall distribution calculated from Table II is used and in four subruns the annual application of 115 kg P ha^{-1} occurs on 31 March, 30 June, 30 September, and 31 December, respectively. The results show that immobilisation of P in the tilled layer is largest if P is applied on 31 March, and the least when applied on 30 September. The resulting differences are, however, so small that they cannot be clearly shown in a figure.

DISCUSSION

The physico-mathematical model presented in this paper can be used to predict effects of surplus application of orthophosphate on the amounts of phosphate dissolved in the soil water, reversibly adsorbed by the solid phase, and immobilised by reactions with aluminum and iron. The expressions for the frontal velocity v_f and the average concentration $\bar{c}_\infty$ summarise the main, long-term features of penetration of phosphate. Equation (1) is similar to the classical relation between the leaching fraction and solute concentrations in irrigation and drainage waters (U.S. Salinity Lab. Staff, 1954). It shows that after the fixation and adsorption capacities are filled, orthophosphate is assumed to behave as chloride.

Our purpose was to estimate to what extent regular dumping of large amounts of orthophosphate will eventually cause harmful contamination of ground and surface water. In this context the concentration of phosphate in the soil solution is the most relevant variable. If values of the half-life of immobilisation are low, i.e., less than 0.02 year, the fixation front is sharp. Ahead of the fixation front the equilibrium value still prevails. Behind the front the average concentration is given by equation (1). Equation (25) of Part I gives the velocity of the fixation front which can be used to estimate when the concentration at a certain depth will start to rise. Thus with a front velocity of 8 mm year^{-1} (Table I) one would expect the concentration at 0.25 and 0.50 m, respectively, to increase after slightly more than 30 and 60 years, which indeed is the case as shown in Figs. 8a and b. With longer half-life and consequently more diffuse fronts the situation is more complicated and results can only be obtained by computer calculations.

In order to predict the effect of leaching of phosphate into the groundwater on the concentration of the surface water, further information is needed on the flow pattern between the water table and drains or ditches. Existing multidimensional transport theory (Raats, 1980) can be used if: (a) the water table is relatively flat; (b) the distance between ditches and tile drains is known and large relative to the depth of the impermeable layer; and (c) the sharp front approximation discussed above is applicable. Otherwise a detailed numerical solution for transport along individual flow lines will be needed. In particular this will be the case if rapid deep penetration is due to slow immobilisation values of $\tau_{1/2}$ (of more than several years), since then the fronts will be very diffuse.

The assumptions made in the model are based on data obtained from experiments representing field conditions as much as possible. However, as phosphate immobilisation kinetics are extremely slow, results from the experiments will always suffer from the fact that one or more parameters will have been altered beyond the range encountered in practice in order to make evaluation within a reasonable timespan possible. Experiments under field conditions used to obtain long-term effects of phosphate applications to soils suffer from the very long duration necessary to obtain useful results.

This makes verification of models such as presented here difficult. In spite of these difficulties it is the view of the authors that computer simulation offers an acceptable way of predicting effects of phosphate pollution within a reasonable margin of error.

In Part III the theory will be used to evaluate data from an acid sandy soil column heavily treated with pig slurry (Gerritse et al., 1982).

REFERENCES

De Wit, C.T. and Van Keulen, H., 1972. Simulation of Transport Processes in Soil. PUDOC, Wageningen, 100 pp.

Gerritse, R.G., De Willigen, P. and Raats, P.A.C., 1982. Transport and fixation of phosphate in acid, homogeneous soils. III. Experimental study of acid, sandy soil columns heavily treated with pig slurry. Agric. Environm., 7: 175—185.

Raats, P.A.C., 1980. Multidimensional transport of solutes in saturated and in unsaturated soils. Neth. J. Agric. Sci., 28: 7—15.

Raats, P.A.C., De Willigen, P. and Gerritse, R.G., 1982. Transport and fixation of phosphate in acid, homogeneous soils. I. Physico-mathematical model. Agric. Environm., 7: 149—160.

Rijtema, P.E. and Bon, J., 1974. Bepaling landbouwkundige gevolgen van grondwaterwinning met behulp van bodemkundige gegevens (Determining the agricultural consequences of pumping groundwater with the aid of soil data). I.C.W. Regionale Studies, No. 7, Instituut voor Cultuurtechniek en Waterhuishouding, Wageningen, 43 pp.

U.S. Salinity Lab. Staff, 1954. Diagnosis and Improvement of Saline and Alkali Soils. U.S. Dep. Agric. Handbook No. 60, Washington, DC, 160 pp.